Applied Physics Letters

Revealing intrinsic electro-optic effect in single domain Pb(Zr, Ti)O_3 thin films

Cite as: Appl. Phys. Lett. **119**, 102902 (2021); https://doi.org/10.1063/5.0056121
Submitted: 06 May 2021 • Accepted: 27 August 2021 • Published Online: 08 September 2021

Shinya Kondo, Tomoaki Yamada, Masahito Yoshino, et al.

Applied Physics Letters ARTICLE scitation.org/journal/apl

Revealing intrinsic electro-optic effect in single domain Pb(Zr, Ti)O_3 thin films

Cite as: Appl. Phys. Lett. **119**, 102902 (2021); doi: 10.1063/5.0056121
Submitted: 6 May 2021 · Accepted: 27 August 2021 ·
Published Online: 8 September 2021

Shinya Kondo,[1,2] Tomoaki Yamada,[1,3,a)] Masahito Yoshino,[1] Takashi Teranishi,[2,4] Akira Kishimoto,[2] and Takanori Nagasaki[1]

AFFILIATIONS

[1]Department of Energy Engineering, Nagoya University, Furo-cho, Chikusa-ku, Nagoya 464-8603, Japan
[2]Graduate School of Natural Science and Technology, Okayama University, 3-1-1 Tsushima-naka, Kita-ku, Okayama 700-8530, Japan
[3]Materials Research Center for Element Strategy (Tokyo Tech MCES), Tokyo Institute of Technology, 4259 Nagatsuta, Midori-ku, Yokohama 226-8502, Japan
[4]Laboratory for Materials and Structures, Tokyo Institute of Technology, 4259 Nagatsuta, Midori-ku, Yokohama 226-8503, Japan

[a)]Author to whom correspondence should be addressed: t-yamada@energy.nagoya-u.ac.jp

ABSTRACT

We deposited polar-axis-oriented tetragonal and rhombohedral single domain Pb(Zr, Ti)O_3 (PZT) films on CaF_2(100) substrates by inserting $SrRuO_3$ (SRO)/$LaNiO_3$ and SRO/$SrTiO_3$/TiO_2/CeO_2 buffer layers. Both PZT films grew epitaxially and had a (001)- and (111)-domain with the remnant polarization and piezoelectric constant comparable to the theoretical values of PZT single crystals having the same compositions. The electro-optic (EO) response of the fabricated PZT films was constant with respect to the DC electric field and increased linearly with an increasing AC electric field, thus representing a typical linear EO response in single domain ferroelectrics. The measured EO coefficients were larger than the value for a single crystal of $PbTiO_3$, i.e., one of the end members of PZT, but smaller than the values reported for polycrystalline and epitaxial PZT films with multiple domains. These findings show that the intrinsic EO effect is enhanced in PZT, which is similar to the enhancement seen in the dielectric and piezoelectric constants. Moreover, most of the reported EO response in PZT films is supported by additional extrinsic contributions.

Recently, the electro-optic (EO) effect in ferroelectric thin films has attracted considerable attention for optical modulators in advanced Si photonics.[1–3] Among the ferroelectric materials, oxides with a perovskite structure, such as $BaTiO_3$, (Pb, La)(Zr, Ti)O_3, and Pb(Zr, Ti)O_3 (PZT), exhibit a large EO coefficient and, thus, are attractive candidates for such devices.[2,4–24] The morphotropic phase boundary (MPB) can be used to increase the EO coefficient of such ferroelectric perovskite oxides, because the dielectric and piezoelectric responses are drastically enhanced near the MPB.[25,26] For example, Zhu *et al.* reported that the linear EO coefficient of polycrystalline PZT films grown on (Pb, La)TiO_3 buffered glass substrates was enlarged by approaching the MPB composition.[21]

The EO response can be classified into three contributions: an intrinsic contribution arising from the polarization extension and rotation, a contribution by the elasto-optic effect, and a contribution arising from the change in the polarization direction due to the ferroelastic domain switching associated with domain wall motion. Among them, the intrinsic EO response is essentially important for fast-growing optical telecommunication applications operating at over tens of GHz frequencies as the ferroelastic domain switching cannot follow at such high frequencies.

The intrinsic EO response is known to be influenced by the polarization-optic (PO) coefficient, which is similar to various perovskite oxides except for Pb-based materials. The PO coefficient of the reported some Pb-based materials is 1/10 or less than that of the coefficient of materials without Pb.[27] Nevertheless, large EO responses were reported not only in the materials without Pb, such as $BaTiO_3$, but also in Pb-based materials, such as PZT, near the MPB.[4,6,8,9,11,12,15–17,21] This suggests that the large EO response in Pb-based materials near the MPB may not have been solely achieved by the enhanced intrinsic effect. However, most studies have been conducted using polycrystalline films or films with a multiple domain structure, thus making it challenging to determine if the EO response is enhanced intrinsically or extrinsically by approaching the MPB.[4–23] It should be noted that PZT with a composition at MPB shows a complex multi-domain state or nano-scale domains even in the epitaxial

films.[28] Therefore, it is crucial to reveal the intrinsic EO response of PZT using the single-domain state for compositions other than MPB. However, the EO coefficient of single domain PZT has only been reported for $PbTiO_3$ (PTO) crystals, i.e., one of the end members of PZT, because of the difficulty in fabricating PZT crystals with high optical quality.[29]

The stress engineering of epitaxial films is useful for revealing the intrinsic EO response of single domain PZTs. By applying a compressive stress to the epitaxial PZT films when crossing the paraelectric-to-ferroelectric phase transition after cooling from the deposition temperature, single domains with (001) and (111) polar-axes can be stabilized for the tetragonal and rhombohedral PZT films. However, the intrinsic EO response is primarily affected by the strain of the films, i.e., the magnitude of EO response is increased or decreased by the magnitude and the sign of the strain.[30–32] Therefore, it is essential to induce the required minimum stress so that the residual strain after the phase transition can be small enough. This can be achieved using CaF_2 as a substrate, which has approximately double the thermal expansion coefficient as that of PZT. The difference in the thermal expansion coefficient between PZT and CaF_2 results in the required minimum compressive stress in the PZT films, thus stabilizing the single domain.[33–36]

In this study, we fabricated (001)-tetragonal and (111)-rhombohedral single domain epitaxial PZT films having out-of-plane polar-axes by inserting buffer layers on CaF_2(100) substrates, and we clarified their intrinsic EO response. By comparing the EO coefficient measured in this study with theoretically estimated values and previously reported experimental values for polycrystalline films and epitaxial films with multiple domains, we show that the intrinsic EO response is enhanced in PZT but the extrinsic contribution could be a significant factor in enhancing the EO response reported in most previously reported film studies.

$Pb(Zr_xTi_{1-x})O_3$ and buffer layers were deposited on CaF_2(100) substrates using pulsed laser deposition (PLD) with a KrF excimer laser (λ = 248 nm, 60 mJ). 494 nm-thick tetragonal ($x = 0.35$) and 660 nm-thick rhombohedral ($x = 0.7$) PZT films were grown on $SrRuO_3$ (SRO)/$LaNiO_3$/CaF_2 and SRO/$SrTiO_3$/TiO_2/CeO_2/CaF_2 at 610 and 630 °C in 200 mTorr O_2, respectively. The reason why the CaF_2(100) substrates were used for the growth of both (001)-tetragonal and (111)-rhombohedral PZT films is their lattice matching. Since the perovskite lattices (PZT, SRO, and $LaNiO_3$) have the lattice constant about $1/\sqrt{2}$ of the fluorite CaF_2 lattice, the perovskite (001) plane is well matched on the fluorite CaF_2 (001) plane with the in-plane rotation angle of 45°. On the other hand, the perovskite (111) plane cannot be matched on the fluorite CaF_2 (111) plane for any in-plane rotation angles. Therefore, the (111) growth on fluorite CaF_2 substrates is not as simple as that on perovskite substrates such as $SrTiO_3$, where the cube-on-cube epitaxial relationship can be achieved. Thus, we inserted SRO/$SrTiO_3$/TiO_2/CeO_2 layers on the CaF_2(100) substrates, which realize the (111) growth of the top SRO layer. The epitaxial relationships between the buffer layers and the substrates are reported elsewhere.[34,35,37] The thickness of the films was larger than 400 nm, for which the lattice mismatch can be fully relaxed during growth; thus, the residual strain in the films is only affected by the difference in the thermal expansion coefficient between PZT and the CaF_2 substrate. Note that the dead layer effect can also be negligible for such large thicknesses. We used a slightly higher deposition temperature for the rhombohedral PZT film to achieve the crystallinity comparable to the tetragonal PZT film (see Fig. S1). Figures 1(a-1) and 1(b-1) present both the hetero-epitaxial structures, and Table S1 lists the detailed deposition conditions and thicknesses for each layer. Here, the uppermost SRO of the buffer layers serves as a bottom electrode, which was inserted for both tetragonal and rhombohedral PZT films to construct the same metal–insulator–metal capacitor structures. Following the PZT deposition, circular platinum top electrodes, which were 100 or 200 μm in diameter and 10 nm in thickness, were fabricated using electron beam evaporation.

The structural properties of the fabricated films were characterized by x-ray diffraction (XRD) using a four-axis diffractometer with Cu-$K_{\alpha 1}$ x rays (Bruker, D8 DISCOVER) and reflection high-energy electron diffraction (RHEED) (PASCAL). The thickness of the PZT films was calculated from the deposition rate determined from cross-sectional images obtained by field emission scanning electron microscopy (Hitachi, S-4800). The dielectric properties and ferroelectric properties of the PZT films were investigated using a precision LCR meter (Keysight, E4980A) and a ferroelectric tester (Toyo, FCE-1), respectively. The converse piezoelectric constant was characterized in the force curve mode using piezoelectric force microscopy (PFM) (Asylum Research, MFP-3D). The EO property of the PZT films was measured by in-house transmission modulation ellipsometry, whose details are described elsewhere.[32] An incident angle and a polarization angle of a polarized He–Ne laser (λ = 632.8 nm) were fixed at 45°. A sinusoidal field E_{AC} at 1 kHz with a DC voltage was applied to the samples. The E_{AC} = 6.4 kV/cm (corresponding to 9.1 kV/cm in peak to peak) was used for the DC field dependence measurements, and a DC field equal to $E_{AC}/2\sqrt{2}$ was used for the AC field dependence measurements in order to avoid the 180° domain switching of PZT films by the alternate electric field and, thus, to ensure the single domain state during the measurement.

Figures 1(a-2) and 1(b-2) show the XRD $2\theta/\omega$ scans of the fabricated tetragonal and rhombohedral PZT films on SRO/$LaNiO_3$/CaF_2 and SRO/$SrTiO_3$/TiO_2/CeO_2/CaF_2, respectively. Both PZT films had a perovskite structure without secondary phases. The RHEED patterns indicated that PZT films with relatively flat surfaces grew epitaxially on the substrates, as shown in Figs. 1(a-3) and 1(b-3). The tetragonal PZT film showed a perfect (001)-orientation without (100)-orientation; namely, the tetragonal film has a *c*-domain structure, where the polar axis is oriented normal to the substrate. The rhombohedral PZT film showed a (111)-orientation with a small amount of (110) and (001)-orientations caused by partial misorientation of the buffer layers. Because the fraction of (110) and (001)-orientations was estimated to be less than 2%, it can be concluded that the rhombohedral film has an almost perfect (111)-orientation. The fact that there is no $(11\bar{1})$-orientation shows that the rhombohedral film has a domain with a polar axis normal to the substrate. These PZT films have comparable crystallinity (Fig. S1) and have epitaxial relationships with the substrate as follows: [110]PZT(001) || [100]CaF_2(001) for PZT/SRO/$LaNiO_3$/CaF_2 and $[01\bar{1}]$PZT(111) || [100]CaF_2(001) for PZT/SRO/$SrTiO_3$/TiO_2/CeO_2/CaF_2 (Fig. S2). XRD reciprocal space mapping around PZT 203 [Fig. 1(c)] and XRD 2θ-χ mapping around PZT 200 [Fig. 1(d)] were performed for the tetragonal and rhombohedral PZT films, respectively, to investigate the residual strain in these PZT films. The in-plane and out-of-plane lattice constants were estimated to be $a = 3.994$ Å and $c = 4.147$ Å for the tetragonal film and

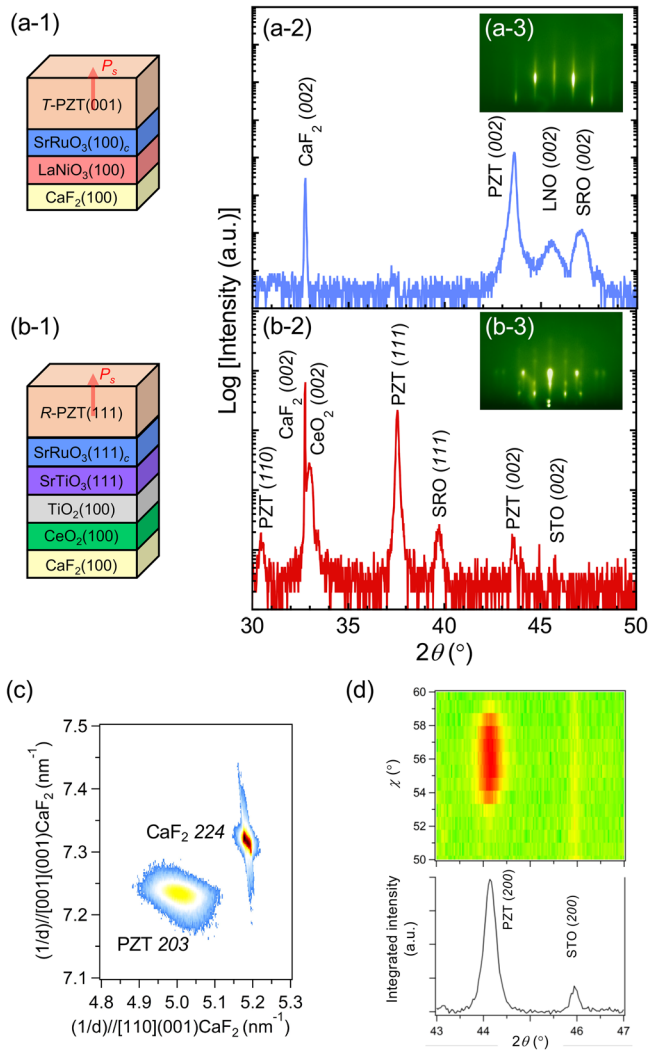

FIG. 1. (1) Schematic illustrations of the fabricated epitaxial structures, (2) XRD $2\theta/\omega$ patterns and (3) RHEED patterns for (a) the tetragonal PZT film and (b) the rhombohedral PZT film. (c) XRD reciprocal space mapping around PZT 203 for the tetragonal PZT film and (d) XRD 2θ-χ mapping and the integrated intensity along the χ direction for the rhombohedral PZT film.

$a = c = 4.100$ Å for the rhombohedral film, which are close to those of bulk PZT [$a = 3.99$ Å and $c = 4.15$ Å for the tetragonal phase ($x = 0.35$) and $a = c = 4.10$ Å for the rhombohedral phase ($x = 0.7$)].[38] This suggests that the residual strain of both fabricated tetragonal and rhombohedral PZT films is negligible. Thus, the fabrication of polar axis orientated PZT films without strain was achieved for both tetragonal and rhombohedral compositions.

Figures 2(a) and 2(b) present the polarization–electric field (P–E) hysteresis loops measured at 1 kHz. Both the hysteresis loops have a well-saturated square shape and showed symmetrical polarization switching behavior to the positive and negative electric fields. The coercive field for the (111)-rhombohedral PZT film was less than that for the (001)-tetragonal PZT film, as reported previously.[33] The remnant polarization and relative dielectric constant at 10 kHz (not shown here) were 60 μC/cm^2 and 136, and 61 μC/cm^2 and 342 for the (001)-tetragonal and (111)-rhombohedral PZT films, respectively, which are in good agreement with the theoretically estimated values of 61 μC/cm^2 and 157, and 65 μC/cm^2 and 280 for bulk single crystals reported by Haun *et al.*[39] This ensures the single domain state of those PZT films under the top electrode after the bias applications. Regarding the piezoelectric property, our previous study showed that the piezoelectric constant d_{33} of the (001)-tetragonal PZT film having the same heteroepitaxial structures was 60–70 pm/V, which is comparable to the clamped bulk single crystal,[34] but that of the (111)-rhombohedral PZT film has not been clarified thus far. Figure 2(c) shows the field-induced displacement of the (111)-rhombohedral PZT film measured by PFM. Although the switching behavior was less abrupt than the (001)-tetragonal PZT film, a clear butterfly loop by polarization switching was observed. In addition, the displacement under the unipolar regime linearly changed with increasing electric field, which is a typical piezoelectric response without extrinsic domain contributions. The d_{33} calculated from the slope of the unipolar regime was 46 pm/V. Within the accuracy of the measurements, it is close to the theoretical value of 57.5 pm/V for bulk single crystals calculated considering the influence of substrate clamping. These results suggest that the fabricated (001)-tetragonal and (111)-rhombohedral PZT films have ferroelectric and piezoelectric properties comparable to those of bulk single crystals.

The DC and AC electric field dependences of the modulation amplitude and phase of light were measured using modulation ellipsometry to clarify the EO properties of the fabricated single domain PZT films. Figures 3(a) and 3(b) show the DC field dependence for the (001)-tetragonal and (111)-rhombohedral PZT films. The phase was changed by 180° by sweeping the DC field for both PZT films, which showed the polarization reversal of both PZT films by the DC field. In addition, a wider hysteresis was observed for the (001)-tetragonal PZT film than the (111)-rhombohedral PZT film, as observed in the P–E hysteresis loops shown in Fig. 2. An obvious hump or nose, which is caused by the field-induced effect or 180° polarization switching under a small E_{AC}, was not observed, because the phase transition temperatures of PZT are far above room temperature.[39] The almost constant amplitude, independent of the applied DC field, was because these films have a single domain.[32] Figure 3(c) shows the AC field dependence for the PZT films. The modulation amplitude changed linearly with the applied AC field for both the tetragonal and rhombohedral PZT films, i.e., these films showed a linear EO response. Thus, the estimated effective EO coefficients, r_c, were nearly constant against the applied AC field. Here, the r_c was estimated as follows. On the basis of the approximation $n \approx n_1 \approx n_3$, where n_1 and n_3 are the principal refractive indices of the PZT films, r_c, can be estimated by the relationship[40–42]

$$r_c = \frac{\lambda I_{AC}}{\pi n^2 V I_{DC}} \cdot \frac{\sqrt{n^2 - \sin^2\theta}}{\sin^2\theta}, \quad (1)$$

where λ, n, V, I_{AC}, and I_{DC} are the wavelength of the He–Ne laser, the refractive index of the PZT films, the applied alternative voltage, and the AC modulation and average intensity of the transmitted light, respectively. The $\frac{I_{AC}}{I_{DC}}$ corresponds to the modulation amplitude shown in Fig. 3(c). n for the PZT films was evaluated using a prism coupler (Metricon, 2010). To reduce the influence of coupling of light into buffer layers, thicker PZT films having an 800-nm thickness were

fabricated. The evaluated n was 2.3 for both tetragonal and rhombohedral PZT films, which was close to but somewhat smaller than the values of epitaxial PZT films from the systematic study by Foster *et al.*[43] Due to the difficulty in accurately taking into account the effect of multiple buffer layers for the estimation of the refractive index of PZT films, we adopted the values reported by Foster *et al.*[43] to evaluate the EO coefficients in the present study. Note that the influence of the difference in the refractive index is minor and does not affect our discussions. The estimated average r_c was 17.9 and 26.8 pm/V for the (001)-tetragonal and (111)-rhombohedral PZT films, respectively.

The EO coefficients measured in this study were compared with those of other values reported for PZT. Figure 4 shows the EO coefficients r_c for PZT as a function of $P_S\varepsilon$, where P_S is the spontaneous polarization and ε is the dielectric constant. For consistency with various experimental reports, the $P_S\varepsilon$ were calculated using the values reported by Haun *et al.*[39,44] The theoretical r_c is estimated for the tetragonal phase using the following equations:

$$r_c = 2\left(g^{S}_{3333} - g^{S}_{1133}\right)P_{S,3}\chi_{33} + \left(p^{P}_{3333} - p^{P}_{1133}\right)d^{f}_{333} \quad (2)$$

$$= 2\left(g^{T}_{3333} - g^{T}_{1133}\right)P_{S,3}\chi_{33} \quad (3)$$

$$d^{f}_{333} = d_{333} - 2\left(s^{E}_{1122}/\left(s^{E}_{1111} + s^{E}_{1122}\right)\right)d_{311}, \quad (4)$$

where g^{S}_{ijkl}, g^{T}_{ijkl}, p^{P}_{ijkl}, χ_{lm}, d^{f}_{mkl}, d_{mkl}, and s^{E}_{ijkl} are the quadratic PO tensor at constant strain and stress, the elasto-optic tensor at constant polarization, the electric susceptibility at low frequencies, the piezoelectric coefficient of clamped film and unclamped bulk, and the elastic compliance at a constant electric field, respectively.[31,32,45] In Eq. (2), the first and second terms describe the intrinsic EO effect and the elasto-optic effect, respectively. Note that χ_{lm} in the first term can be regarded as ε_{lm} for simplicity because of $\chi_{lm} \gg 1$. Unfortunately, the g^{S}_{ijkl} and p^{P}_{ijkl} have been reported only for two end members of PZT: $PbTiO_3$ (PTO) and $PbZrO_3$ (PZO).[29,46,47] The latter is antiferroelectric; thus, the interpolation from those values to find g^{S}_{ijkl} and p^{P}_{ijkl} for PZT may not be appropriate. In addition, experimentally determined g^{S}_{ijkl} for PTO was reported to be negative, even though it is generally positive for most perovskite materials.[47] Therefore, in this study, the quadratic PO tensor at constant stress, g^{T}_{ijkl}, was calculated from the measured r_c of the PTO single crystal using the calculated $P_{S,3}\chi_{33}$.[29] Note that g^{T}_{ijkl} involves the elasto-optic effect as seen in Eq. (3). The theoretical line using the estimated g^{T}_{ijkl} is drawn for the tetragonal phase in the figure.

The measured r_c of the tetragonal and rhombohedral PZT films with a single domain was larger than the r_c of a PTO single crystal (8.11 pm/V),[29] even though the elasto-optic effect was suppressed in the films by substrate clamping [see Eq. (4)]. Note that the influence of the suppression of the elasto-optic effect in a clamped PTO film on the total EO response can be predicted to be less than 10% using the reported coefficients.[29,39,44,47,48] This clearly shows that the intrinsic EO response is enhanced in PZT. Interestingly, the measured r_c of our PZT films are approximately on the theoretical solid line based on the coefficients of PTO, suggesting that the enhanced intrinsic EO response in PZT is caused by the larger $P_S\varepsilon$ rather than the larger g^{T}_{ijkl} compared to PTO. Jiang *et al.* reported that the EO coefficient r_{33} was calculated to be 11.9 pm/V for PZT ($x = 0.52$) at 0 K by *ab initio* calculations, which also supports the experimental finding that the EO response of single domain PZT is larger than that of PTO but remains below a few tens pm/V.[49]

The majority of the reported r_c of the PZT films were larger than that for the PTO single crystal and the single domain PZT films in the present study. Note that the reported PZT films are either polycrystalline or epitaxial with multiple domains or with an MPB phase, where the nano-scale domains are inherent. Although there were significant variations in the reported r_c, even for the same compositions, there was a clear tendency that the PZT films near the MPB show larger r_c than those in tetragonal and rhombohedral phases. One possible reason for the variation in r_c is the structural quality of the fabricated films.[24] A more probable reason is the extrinsic contribution by the change in the polarization direction, such as non-180° ferroelastic domain switching associated with domain wall motion. The polycrystalline films and epitaxial films with multiple domains or with the MPB phase have several possible polar directions, in which the polarization can be reoriented using an external electric field. The direction of such a polarization change induces a change in the refractive indices with respect to the polarization of the light. Guilbert *et al.* reported that an electric field could tilt the optical indicatrix in $RbHSeO_4$ crystals; thus, the EO response was enhanced by dynamic field-induced domain reversals.[50] Apart from the EO response, similar enhancement

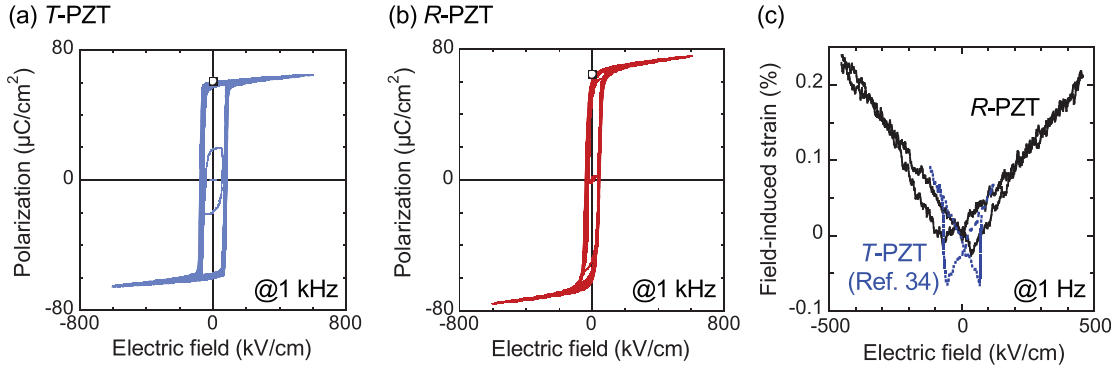

FIG. 2. *P–E* hysteresis loops measured at 1 kHz for (a) the (001)-tetragonal PZT film and (b) the (111)-rhombohedral PZT film. The square symbol in the figures shows the theoretically estimated spontaneous polarization values of bulk crystals reported by Haun *et al.*[39] (c) Field-induced displacement for the (111)-rhombohedral PZT film measured by PFM at 1 Hz. The dashed line also plots the previous data for the (001)-tetragonal PZT film (Ref. 34).

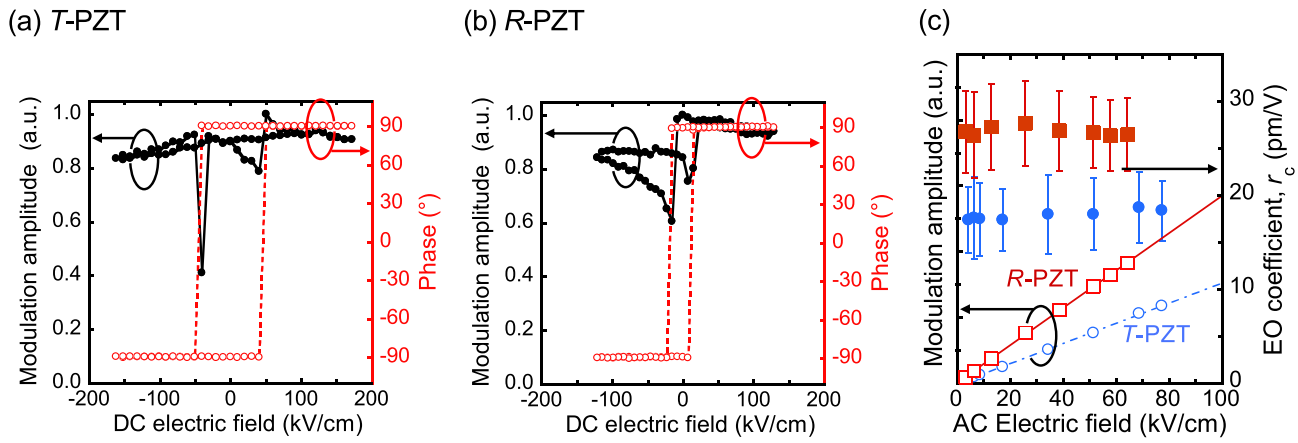

FIG. 3. DC electric field dependence of the modulation amplitude and phase for (a) the (001)-tetragonal PZT film and (b) the (111)-rhombohedral PZT film. (c) AC electric field dependence of the modulation amplitude and the EO coefficient r_c.

is well known for the piezoelectric response. Cao *et al.* performed a phase-field simulation of the PZT single crystal near the MPB and reported that the piezoelectric response could be enhanced by the change in the polarization direction.[51] Although the systematic comparison between single and multi-domain epitaxial PZT films is needed to clarify the detailed extrinsic contribution to the EO response in the future, the reported large EO coefficients over the theoretical line are likely due to such an extrinsic contribution.

In summary, (001)-tetragonal and (111)-rhombohedral PZT films were fabricated on CaF_2(100) substrates by PLD. The fabricated PZT films had a single domain with negligible residual strain and exhibited ferroelectric and piezoelectric properties equivalent to those of clamped bulk single crystals. The EO coefficients were 17.9 and 26.8 pm/V for the tetragonal and rhombohedral PZT films, respectively, indicating an enhanced intrinsic EO response arising from the larger $P_S\varepsilon$ than PTO. Finally, a comparison with the reported EO response of the polycrystalline PZT films and epitaxial PZT films with multiple domains or with the MPB phase suggested that the additional extrinsic contributions strengthen the large EO responses reported in such PZT films.

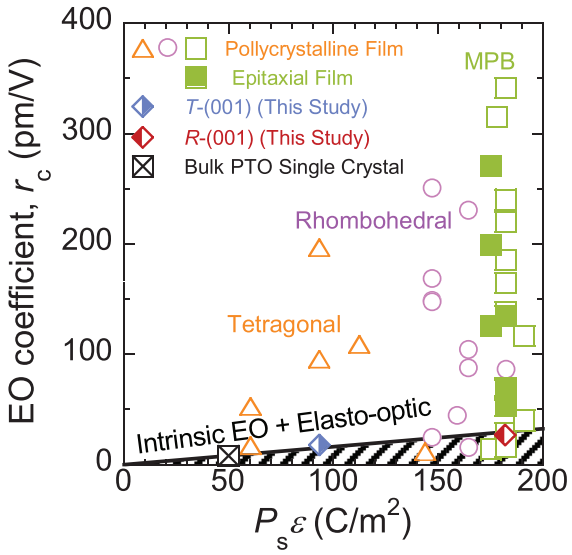

FIG. 4. Comparison of the EO coefficients r_c for the tetragonal and rhombohedral single domain PZT films in this study, the previously reported PTO single crystal, polycrystalline PZT films, and epitaxial PZT films with multiple domains or with the MPB phase, as a function of $P_S\varepsilon$.[4–23,29] The solid line shows the theoretically estimated r_c for the tetragonal phase.

See the supplementary material for the deposition conditions, layer thickness, crystallinity, and epitaxial relationships of the heteroepitaxial structures fabricated in this study.

This work was supported partly by the JSPS KAKENHI (Grant No. 19J12654) (S.K.), the Murata Science Foundation (T.Y.), the Foundation of Public Interest of Tatematsu (T.Y.), and MEXT Element Strategy Initiative to Form Core Research Center (Grant No. JPMXP0112101001) (T.Y.).

DATA AVAILABILITY

The data that support the findings of this study are available within the article and its supplementary material.

REFERENCES

[1]F. Eltes, C. Mai, D. Caimi, M. Kroh, Y. Popoff, G. Winzer, D. Petousi, S. Lischke, J. E. Ortmann, L. Czornomaz, L. Zimmermann, J. Fompeyrine, and S. Abel, J. Lightwave Technol. **37**, 1456 (2019).
[2]S. Abel, F. Eltes, J. E. Ortmann, A. Messner, P. Castera, T. Wagner, D. Urbonas, A. Rosa, A. M. Gutierrez, D. Tulli, P. Ma, B. Baeuerle, A. Josten, W. Heni, D. Caimi, L. Czornomaz, A. A. Demkov, J. Leuthold, P. Sanchis, and J. Fompeyrine, Nat. Mater. **18**, 42 (2019).
[3]A. Messner, F. Eltes, P. Ma, S. Abel, B. Baeuerle, A. Josten, W. Heni, D. Caimi, J. Fompeyrine, and J. Leuthold, J. Lightwave Technol. **37**, 281 (2019).
[4]C. Lee, V. Spirin, H. Song, and K. No, Thin Solid Films **340**, 242 (1999).
[5]H.-S. Kang and W.-J. Lee, J. Vac. Sci. Technol. A **20**, 1498 (2002).
[6]G. Teowee, J. T. Simpson, T. Zhao, M. Mansuripur, J. M. Boulton, and D. R. Uhlmann, Microelectron. Eng. **29**, 327 (1995).
[7]K. Nashimoto, S. Nakamura, T. Morikawa, H. Moriyama, M. Watanabe, and E. Osakabe, Jpn. J. Appl. Phys., Part 1 **38**, 5641 (1999).
[8]M. M. Zhu, Z. H. Du, and J. Ma, J. Appl. Phys. **108**, 113119 (2010).

[9]S. Masuda, A. Seki, and Y. Masuda, Appl. Phys. Lett. **96**, 072901 (2010).
[10]H. Shima, H. Naganuma, and S. Okamura, Jpn. J. Appl. Phys., Part 1 **45**, 7279 (2006).
[11]J. P. George, P. F. Smet, J. Botterman, V. Bliznuk, W. Woestenborghs, D. V. Thourhout, K. Neyts, and J. Beeckman, ACS Appl. Mater. Interfaces **7**, 13350 (2015).
[12]T. D. Kang, B. Xiao, V. Avrutin, Ü. Özgür, H. Morkoç, J. W. Park, H. S. Lee, H. Lee, X. Wang, and D. J. Smith, J. Appl. Phys. **104**, 093103 (2008).
[13]C. V. R. V. Kumar, M. Sayer, R. Pascual, D. T. Amm, Z. Wu, and D. M. Swanston, Appl. Phys. Lett. **58**, 1161 (1991).
[14]C. E. Land, J. Am. Ceram. Soc. **72**, 2059 (1989).
[15]V. V. Spirin, C. Lee, and K. No, J. Opt. Soc. Am. B **15**, 1940 (1998).
[16]M. Zhu, Z. Du, L. Jing, A. I. Y. Tok, and E. H. T. Teo, Appl. Phys. Lett. **107**, 031907 (2015).
[17]M. M. Zhu, Z. H. Du, and J. Ma, J. Appl. Phys. **106**, 023113 (2009).
[18]M. Nakada, K. Ohashi, and J. Akedo, J. Cryst. Growth **275**, e1275 (2005).
[19]G. Yi, Z. Wu, and M. Sayer, J. Appl. Phys. **64**, 2717 (1988).
[20]M. Zhu, Z. Du, S. S. Chng, S. H. Tsang, and E. H. T. Teo, J. Mater. Chem. C **6**, 12919 (2018).
[21]M. Zhu, H. Zhang, Z. Du, and C. Liu, Ceram. Int. **45**, 22324 (2019).
[22]L. Chen, Y. Zhang, Q. Guo, D. Zhang, X. Zhong, and J. Yuan, Appl. Phys. Lett. **105**, 112903 (2014).
[23]J.-J. Choi, G.-T. Park, H.-E. Kim, and D.-Y. Kim, Thin Solid Films **515**, 2437 (2006).
[24]K. J. Kormondy, Y. Popoff, M. Sousa, F. Eltes, D. Caimi, M. D. Rossell, M. Fiebig, P. Hoffmann, C. Marchiori, M. Reinke, M. Trassin, A. A. Demkov, J. Fompeyrine, and S. Abel, Nanotechnology **28**, 075706 (2017).
[25]X. Qian, H. Ye, Y. Zhang, H. Gu, X. Li, C. A. Randall, and Q. M. Zhang, Adv. Funct. Mater. **24**, 1300 (2014).
[26]Y. Barad, Y. Lu, Z.-Y. Cheng, S.-E. Park, and Q. M. Zhang, Appl. Phys. Lett. **77**, 1247 (2000).
[27]P. D. Thacher, J. Appl. Phys. **41**, 4790 (1970).
[28]T. Asada and Y. Koyama, Phys. Rev. B **75**, 214111 (2007).
[29]M. D. Fontana, F. Abdi, and K. Wojcik, J. Appl. Phys. **77**, 2102 (1995).
[30]C. Paillard, S. Prokhorenko, and L. Bellaiche, npj Comput. Mater. **5**, 6 (2019).
[31]S. Kondo, T. Yamada, A. Tagantsev, N. Setter, M. Yoshino, and T. Nagasaki, J. Ceram. Soc. Jpn. **127**, 348 (2019).
[32]S. Kondo, T. Yamada, A. K. Tagantsev, P. Ma, J. Leuthold, P. Martelli, P. Boffi, M. Martinelli, M. Yoshino, and T. Nagasaki, Appl. Phys. Lett. **115**, 092901 (2019).
[33]Y. Ehara, S. Utsugi, T. Oikawa, T. Yamada, and H. Funakubo, Jpn. J. Appl. Phys., Part 1 **53**, 04ED06 (2014).
[34]T. Fujisawa, H. Nakaki, R. Ikariyama, T. Yamada, M. Ishikawa, H. Morioka, and H. Funakubo, J. Appl. Phys. **105**, 061614 (2009).
[35]Y. Ehara, T. Oikawa, T. Yamada, and H. Funakubo, Jpn. J. Appl. Phys., Part 1 **52**, 09KA02 (2013).
[36]T. Fujisawa, H. Nakaki, R. Ikariyama, H. Morioka, T. Yamada, K. Saito, and H. Funakubo, Appl. Phys. Express **1**, 085001 (2008).
[37]T. Yamada, N. Wakiya, K. Shinozaki, and N. Mizutani, Appl. Phys. Lett. **83**, 4815 (2003).
[38]K. Kakegawa, J. Mouri, K. Takahashi, H. Yamamura, and S. Shirasaki, Nippon Kagaku Kaishi **1976**, 717 (in Japanese).
[39]M. J. Haun, E. Furman, S. J. Jang, and L. E. Cross, Ferroelectrics **99**, 63 (1989).
[40]Y. Levy, M. Dumont, E. Chastaing, P. Robin, P.-A. Chollet, G. Gadret, and F. Kajzar, Mol. Cryst. Liq. Cryst. Sci. Technol., Sect. B **4**, 1 (1993).
[41]S. H. Han and J. W. Wu, J. Opt. Soc. Am. B **14**, 1131 (1997).
[42]C. B. Ma, D. Xu, Q. Ren, Z. H. Lv, H. L. Yang, F. Q. Meng, G. H. Zhang, S. Y. Guo, L. X. Sang, and Z. G. Wang, J. Mater. Sci. Lett. **22**, 49 (2003).
[43]C. M. Foster, G.-R. Bai, R. Csencsits, J. Vetrone, R. Jammy, L. A. Wills, E. Carr, and J. Amano, J. Appl. Phys. **81**, 2349 (1997).
[44]M. J. Haun, Z. Q. Zhuang, E. Furman, S. J. Jang, and L. E. Cross, Ferroelectrics **99**, 45 (1989).
[45]P. Bernasconi, M. Zgonik, and P. Günter, J. Appl. Phys. **78**, 2651 (1995).
[46]R. W. Whatmore and A. M. Glazer, J. Phys. C **12**, 1505 (1979).
[47]S. A. Mabud and A. M. Glazer, J. Appl. Crystallogr. **12**, 49 (1979).
[48]N. A. Pertsev, A. G. Zembilgotov, and A. K. Tagantsev, Phys. Rev. Lett. **80**, 1988 (1998).
[49]Z. Jiang, C. Paillard, H. Xiang, and L. Bellaiche, Phys. Rev. Lett. **125**, 017401 (2020).
[50]L. Guilbert, J. P. Salvestrini, M. D. Fontana, and Z. Czapla, Phys. Rev. B **58**, 2523 (1998).
[51]Y. Cao, G. Sheng, J. X. Zhang, S. Choudhury, Y. L. Li, C. A. Randall, and L. Q. Chen, Appl. Phys. Lett. **97**, 252904 (2010).